Development of Efficient Baroclinic Cooling Prescription for Global Core Collapse Simulations into Protoplanetary Disks

Aaron F. Wienkers[1,3]†, Andrew J. Cunningham[2], Richard I. Klein[2,3], Philip S. Marcus[1], and Christopher F. McKee[2]

[1]Department of Mechanical Engineering, University of California, Berkeley, CA 94720, USA

[2]Department of Astronomy, University of California, Berkeley, CA 94720, USA

[3]Lawrence Livermore National Laboratory, Livermore, CA, 94550, USA

(Fall 2014)

Late protostellar accretion disks are often idealized as thin, Keplerian, and laminar in nature; however, many disk instabilities are not insensitive to the initial turbulence spectrum. One such mode of turbulence driving in protostellar disks is by anisotropic core accretion. We build on the results of Gammie (2001), Rice *et al.* (2005), and Steiman-Cameron *et al.* (2013), now conducting global core collapse simulations with free accretion. We investigate the effects of heavy anisotropic accretion on fragmentation and the proliferation of gravitational instabilities into a gravito-turbulent state. We use the adaptive mesh refinement (AMR) code, *Orion*, to perform high-resolution simulations of solar mass star-forming molecular cloud cores located in massive star-forming regions. We include self-gravity, use a baroclinic equation of state, and represent regions exceeding the maximum grid resolution with sink particles, accurately simulating Bondi accretion. The turbulence, fragmentation, and laminarization of the ensuing late protostellar and early protoplanetary disk is studied during periods of high mass-infall rates. We also outline the development of a global baroclinic cooling prescription for these core collapse simulations forming T Tauri protostellar systems. Our model self-consistently treats the viscously heated disk equilibrium temperature and cooling time using global disk properties. These results will be used to initialize a culminating study of baroclinic instabilities in protoplanetary disks.

Key words: accretion disks — solar system: formation — stars: formation — turbulent flows: rotating turbulence

1. Introduction

Mass and angular momentum transport through accretion disk dead zones have necessitated a purely hydrodynamic instability, motivating recent interest in baroclinic instabilities. Utilizing a baroclinic equation of state—where isopycnals and isobars are allowed the freedom to vary relative to each other (Tritton & Davies 1985)—has already opened up droves of new atmospheric, oceanic, and accretion disk cyclogenic instabilities (Marcus *et al.* 2013; Pedlosky 1987; Ryu & Goodman 1992; Lesur & Papaloizou

† Email address for correspondence: aaron.wienkers@berkeley.edu

2010; Klahr & Bodenheimer 2003). Yet there is still a large disconnect between scientists studying the local evolution of disks, and those looking at their nebular origins.

Local disk simulations are often initialized with an artificial turbulence spectrum in an otherwise ideal Keplerian disk, with little consideration of its origin. The enshrouded nascent disk preceding this T Tauri system seems to be the missing piece between a turbulent molecular cloud core and its late progenitor: a thin, ideal Keplerian protoplanetary disk. Even though this critical transitional period dictates the feasibility of protoplanetary disk initial conditions, the relative laminarization and turbulence dissipation time scales due to rapid accretion is not well studied.

In this paper, we present the adaptive mesh refinement (AMR) hydrodynamic simulation results modeling the formation of a baroclinic protostellar accretion disk from its initial turbulent core collapse through the T Tauri protostellar system using the *Orion* code (Truelove *et al.* 1997, 1998; Klein 1999; Krumholz *et al.* 2007). We focus on the driving of disk turbulence by anisotropic accretion onto a baroclinic disk during the period of rapid accretion, since once accretion onto the protostellar disk has stopped, laminarization is inevitable. The role of this realistic accretion onto the disk in seeding or inhibiting disk instabilities is also investigated. The accretion rate and period during which the disk resembles an ideal Keplerian disk will suggest more realistic initial conditions for local disk simulations.

2. Simulation Setup

2.1. *Solution of Governing Equations*

Our simulations solve the conservative set of gravito-hydrodynamic equations utilizing a spatially and temporally second-order accurate Godunov scheme. The gravito-hydrodynamic equations describing mass, momentum, and energy conservation are respectively

$$\frac{\partial \rho}{\partial t} = -\nabla \cdot (\rho \mathbf{v}) - \sum_i \dot{M}_i W(\mathbf{x} - \mathbf{x}_i) \tag{2.1}$$

$$\frac{\partial}{\partial t}(\rho \mathbf{v}) = -\nabla \cdot (\rho \mathbf{v}\mathbf{v}) - \nabla p - \rho \nabla \phi - \sum_i \dot{\mathbf{p}}_i W(\mathbf{x} - \mathbf{x}_i) \tag{2.2}$$

$$\frac{\partial}{\partial t}(\rho e) = -\nabla \cdot [(\rho e + p)\mathbf{v}] + \rho \mathbf{v} \cdot \nabla \phi - \rho c_v \frac{T - T_{\rm eq}}{t_{\rm cool}} - \sum_i \dot{E}_i W(\mathbf{x} - \mathbf{x}_i) \tag{2.3}$$

where $\mathbf{v}$ is the velocity, p the thermal pressure, ϕ is the gravitational potential, and e the energy density. Energy is removed from Equation 2.3 according to the cooling scheme which will be described in more detail in Section 2.4.

Sink particle mass, momentum, and energy evolution are described by $\dot{M}_i$, $\dot{\mathbf{p}}_i$, and $\dot{E}_i$, where the weighting function, $W(\mathbf{x})$, governs the gas-particle interaction length scale. The gravitational potential is found by solution of the Poisson equation which includes the contribution of each sink particle,

$$\nabla^2 \phi = 4\pi G \left[\rho + \sum_i M_i \delta(\mathbf{x} - \mathbf{x}_i) \right]. \tag{2.4}$$

Finally, an ideal gas equation of state is used with a specific heats ratio of 5/3, appropriate for a cool molecular hydrogen gas too cool to be rotationally excited.

2.2. *Initial and Boundary Conditions*

The initial conditions are chosen to correspond with the formation of a solar-mass star in a region of massive star formation. Although these systems are more common, this does not agree observationally with the initial conditions astronomers see, due to an observational bias whereby low-mass star forming regions are optically thinner.

Our initial model is fully specified by three parameters: the core mass M_c, initial volume-averaged core surface density Σ_c, and the density distribution index k_ρ. These values dictate the dependent parameters of initial core radius and free-fall time, given by

$$R_c = \sqrt{\frac{M_c}{\pi\Sigma_c}} \tag{2.5}$$

and

$$t_{\rm ff} = \left[\frac{\pi M_c}{64G^2\Sigma_c^3}\right]^{1/4}. \tag{2.6}$$

Observations of Infrared Dark Clouds suggest surface densities ranging from $\Sigma_c \sim\ 0.1\,\mathrm{g\,cm^{-2}}$ in diffuse clouds (Evans *et al.* 2009) to $\Sigma_c \sim 1.0\,\mathrm{g\,cm^{-2}}$ (Beuther *et al.* 2002; Rathborne *et al.* 2006). We have chosen to evolve a $M_c = 1.5M_\odot$ core with a typical surface density of $\Sigma_c \sim 0.65\,\mathrm{g\,cm^{-2}}$, for similarity to the local Spectral simulations by Marcus *et al.* (2013). Additionally, the initial core has a power-law density profile of

$$\rho(r) \propto r^{-k_\rho}$$

with $k_\rho = 3/2$ and a core temperature, $T_c = 20$ K, consistent with a supersonically turbulent molecular cloud in free fall, as well as with observation (McKee & Tan 2002, 2003; Beuther *et al.* 2007).

The core is allowed to evolve in a quiescent periodic domain with side length of $6R_c$ to emulate the gravitational effects by the rest of the star cluster. To prevent ambient gas from contributing to the disk turbulence and central object mass, the gas density is set to 0.01 times the density at the edge of the core. Hydrostatic equilibrium between the core and ambient is maintained by setting the temperature of the environment to be 100 times that at the core edge, or 2000 K. Passively advected tracers are used to prevent cooling of the hot ambient gas which would quickly break this equilibrium.

A three-dimensional normalized Gaussian random field is generated (Dubinski *et al.* 1995) with a power spectrum,

$$P(k) \propto k^{-2},$$

consistent with supersonic turbulence. The minimum wavenumber is chosen such that the smallest mode has a wavelength equal to the diameter of the initial core. The magnitude of these velocity perturbations are set by the velocity dispersion,

$$\sigma_v = \sqrt{\frac{GM_c}{2(k_\rho - 1)R_c}} = \left[\frac{G^2 M_c \pi\Sigma_c}{4(k_\rho - 1)^2}\right]^{1/4}, \tag{2.7}$$

which is chosen such that the virial parameter,

$$\alpha_{\rm vir} = \frac{5\sigma_v^2 R_c}{GM_c} = 5. \tag{2.8}$$

Since this value is slightly larger than 15/4 for a core in hydrostatic equilibrium (McKee & Tan 2003) the core initially has greater kinetic energy compared to gravitational energy before the turbulence is allowed to decay. The turbulent crossing time using these parameters, $t_{\rm turb} = 16.8$ kyr, is comparable to the core surface free fall time, $t_{\rm ff} = 18.7$ kyr, and so although the disk will be anisotropically accreting from the core, the initial turbulence will have nearly dissipated. This velocity dispersion is then consistent with the results of McKee & Tan (2003), and forms a supersonically turbulent ($v = 2.1c_s$) and therefore clumpy collapsing initial core. Compared to initializing local disk turbulence directly, our evolved disk has less knowledge of the initial artificial turbulence, and thus should be more realistic.

2.3. *Refinement Criteria*

The simulation domain was discretized onto a 384^3 uniform base-grid. To ensure a broad spectrum of the initial turbulence is resolved, the entirety of the 2500 au core is refined two additional levels, such that 512 cells cover the turbulent collapsing core. Further refinement is necessitated based on the local Jeans number, $J = \sqrt{G\rho\Delta x^2/(\pi c_s^2)}$. Refinement is triggered wherever the local resolution is unable to accurately simulate the high density, where $J > 0.125$ (Truelove *et al.* 1998). Using three additional levels of refinement allows an effective grid scale of $\Delta x_L = 2.5$ AU. Refinement is also forced within a sphere of 300 au, 600 au, and 1000 au for the highest three levels, respectively, to ensure the entirety of the disk and critical accreting matter is refined to 2.5 au. Finally, temporal refinement is proportionate to spatial refinement, and is also chosen to ensure stability by satisfying a Courant number of 0.4.

2.4. *Cooling Prescription*

Common cooling methods in global molecular cloud core simulations include using an isothermal equation of state or employing "barotropic" cooling (Matsumoto & Hanawa 2003; Offner *et al.* 2008; Hansen *et al.* 2012). These simple cooling mechanisms shift the computational efforts to increasing resolution and evolution time, with the caveat that an isothermal disk prevents baroclinicity ($\nabla T \times \nabla \rho = 0$), and an adiabatic disk has unrealistically high temperatures producing a thermally supported accretion disk. The proposed cooling allows the core and disk to evolve baroclinically with more realistic cooling. The baroclinic tern, $\nabla p \times \nabla \rho$, is no longer suppressed due to an isothermal equation of state, and the disk is allowed to evolve with more realistic gas temperatures (see Tritton & Davies (1985) for more discussion on baroclinicity).

In order to isolate the deviations from an ideal Keplerian disk to the effects from anisotropic core accretion, a realistic global Newtonian cooling prescription was chosen to suppress disk fragmentation due to gravitational instability. In this way, a controlled study of disk turbulence driven by accretion can be conducted while maintaining consistency with the continuing spectral simulations by Marcus *et al.* Disk fragmentation studies by Gammie (2001) found a critical cooling time, $t_{\rm cool} \gtrsim 3\Omega^{-1}$, needed for the disk to reach a steady gravitoturbulent state where cooling balances heating due to turbulent dissipation. Thus if cooling is fast relative to the local orbital time, the disk fragments as the Toomre Q drops below unity. In the opposing limit of a long cooling time, or adiabatic core, a thermally supported disk would also contribute to deviations from Keplerian rotation and so is undesirable. Many others have used similar cooling times (Rice *et al.* 2005; Mejia *et al.* 2005; Boley *et al.* 2006), with the assumption that artificial viscosity is small relative to the gravito-turbulent heating. However, as the *Orion* code has numerical viscosity that overwhelms the heating by gravitational instabilities, we must balance energy with viscous heating linearizing the radiative cooling term. Fragmentation is still avoided, since Matzner & Levin (2005) have shown that this viscous heating in protostellar disks around low-mass stars is sufficient to stabilize against fragmentation.

The equilibrium disk temperature is found by balancing energy in an actively heated disk. During the period of interest in the rapid accretion onto a transitional disk, heating is still dominated by viscous dissipation. Protostellar irradiation effects prevalent in a passive disk (Chiang & Goldreich 1997) are thus ignored in the early stages of our disk evolution. Ciesla & Cuzzi (2006) give the effective photospheric temperature of a viscously heated blackbody disk as

$$2\sigma T_{\rm eff}^4 = \frac{9\nu\Sigma\Omega^2}{4}. \tag{2.9}$$

Approximating the disk as steady, so that the equilibrium accretion rate becomes (Alibert *et al.* 2005)

$$\dot{M} = 3\pi\nu\Sigma, \tag{2.10}$$

and using the Eddington approximation for a plane gray atmosphere in local thermodynamic equilibrium, $T_{\rm disk}^4 = \tau T_{\rm eff}^4$, the equilibrium disk temperature can be written as

$$T_{\rm disk}^4 = \frac{3}{16\pi\sigma}\dot{M}\Omega_k^2\kappa_R\Sigma, \tag{2.11}$$

where looking into the midplane of the disk the optical depth is $\tau = \frac{\kappa_R\Sigma}{2}$. Here a power-law approximation of the Rosseland mean dust opacity is used as $\kappa_R \simeq \kappa_0\left(\frac{T}{300\mathrm{K}}\right)^\eta$ where for the temperature range of interest, 20 K to 500 K, $\kappa_0 = 4.8\,\mathrm{cm^2\,g^{-1}}$ and $\eta = 0.8$. A precise empirical opacity is not used here because in reality, the opacity also varies off of the midplane of the disk with the temperature, which cannot be accounted for in these scaling arguments. The weak dependence of the equilibrium temperature on opacity also suggests this approximation has a small effect on the disk thermodynamics.

The column density now must be determined in a self-consistent way from the cooling prescription in order to determine the midplane temperature. Using the disk temperature scaling (2.11), along with the Shakura & Sunyaev (1973) formalism of the alpha viscosity law, $\nu \propto T\Omega^{-1}$, and the equilibrium accretion rate (2.10), the surface density profile is found to scale as

$$\Sigma \propto r^{-\frac{3}{2}\frac{2-\eta}{5-\eta}} = r^{-3/7}$$

for $\eta = 0.8$. This is the consistent solution for a steady alpha disk heated solely by viscous dissipation. Integrating over the disk to determine the disk mass which can be extracted from the simulation, the surface density is found to be

$$\Sigma = \frac{11}{14\pi}r^{-3/7}r_{\rm disk}^{-11/7}\cdot M_{\rm disk}, \tag{2.12}$$

where $r_{\rm disk}$ is defined by the extent of optical thickness perpendicular to the disk.

Thus we are able to approximate the temperature profile of the actively heated transitional disk using only global disk and sink properties. Each of $M_{\rm disk}$, M_*, and $\dot{M}$ are averaged over $t_{\rm ff}/20$, or about 1 kyr, to mitigate unrealistic global thermal oscillations that would occur when the clumpy core gas accretes onto the sink particle.

Our heuristic to define the edge of the disk where $\tau \sim 1$ to the midplane is motivated by the disk thermal time increasing beyond this threshold. The critical densities designating the disk boundaries using the scale heights with and without self-gravity are respectively

$$\rho_{\rm SG} = \frac{\pi G\Sigma_{\rm crit}^2}{2k_bT_{\rm core}/\mu}, \tag{2.13}$$

$$\rho_{\rm NSG}(r) = \sqrt{\frac{GM_*\Sigma_{\rm crit}^2}{2\pi k_bT_{\rm core}r^3/\mu}} \tag{2.14}$$

where $\Sigma_{\rm crit} = 2/\kappa_R(20\mathrm{K}) \sim 4.8$. The disk edge density is then defined as the sum of these

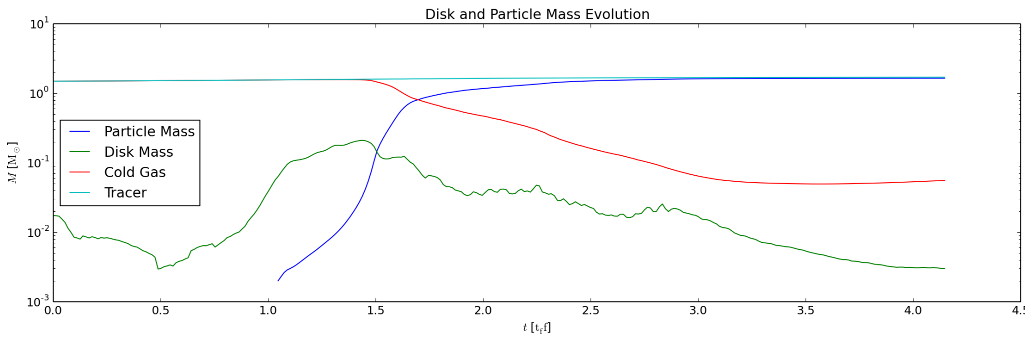

FIGURE 1. Mass evolution of the described system up to protostellar burn.

two in order to capture both regimes with a low-mass disk and a massive self-gravitating disk.

The cooling time consistent with the energy balance (2.11) is found by radiating away the disk energy at T_{eff} to give

$$t_{\mathrm{cool}} = \frac{\frac{1}{2}\Sigma c_v T_{\mathrm{disk}}}{\sigma T_{\mathrm{eff}}^4} = \frac{\Sigma k_b \tau}{2\mu(\gamma-1)\sigma T_{\mathrm{disk}}^3}. \tag{2.15}$$

Using the scaling relations for the opacity and surface density, the disk equilibrium temperature is found to scale with radius as $r^{-15/14}$ for $\eta = 0.8$. Likewise, the cooling time scales as $r^{3/2}$, similar to the cooling proposed by Gammie (2001) only by coincidence, however, since we have not assumed a constant dust opacity here.

To prevent the infalling core from being thermally supported, the core cooling time is set equal to the thermal timescale for a transparent perfectly coupled dusty gas. Taylor expanding the radiative power loss around T_{eq} to first order to match Newtonian cooling gives

$$\left.\frac{de}{dt}\right|_{\mathrm{Newton}} = c_v \frac{T_{\mathrm{c}} - T_{\mathrm{eq}}}{t_{\mathrm{cool,c}}} \simeq 4\kappa\sigma\left(T_{\mathrm{c}}^4 - T_{\mathrm{eq}}^4\right) = \left.\frac{de}{dt}\right|_{\mathrm{S-B}} \tag{2.16}$$

$$t_{\mathrm{cool,c}} = \frac{c_v}{16\kappa(20\mathrm{K})\sigma T_{\mathrm{eq}}^3} \sim 0.6 \text{ years}, \tag{2.17}$$

where both κ and T_{eq} are evaluated far from the sink, where $T \to 20$K. The cooling time is transitioned linearly from the disk cooling (Equation 2.15) at $\rho_{\mathrm{edge}} = \rho_{\mathrm{NSG}} + \rho_{\mathrm{SG}}$ to core cooling at $\rho_{\mathrm{edge}}/2$ as the extents of the disk become optically thin.

These initial conditions and modeled physics suggest relative timescales for our initial molecular cloud core:

$$t_{\mathrm{ff,local}}(r) = \frac{1}{2}\sqrt{\frac{R_c^3}{GM_c}}\left(\frac{r}{R_c}\right)^{k_\rho/2} \sim 23.4\, r_{\mathrm{au}}^{3/4} \text{ yr}, \tag{2.18}$$

$$t_{\mathrm{disk}}(r) = 2\pi\sqrt{\frac{r^3}{GM_*}} \sim r_{\mathrm{au}}^{3/2} \text{ yr}, \tag{2.19}$$

$$\frac{t_{\mathrm{cool}}}{t_{\mathrm{disk}}} \simeq 1.18 \cdot 10^{-4} \left(\frac{M_*}{M_\odot}\right)^{-\frac{3}{16}} \left(\frac{\dot{M}_*}{M_\odot/\mathrm{yr}}\right)^{-\frac{11}{16}} \left(\frac{M_{\mathrm{disk}}}{M_\odot}\right)^{-\frac{21}{16}} \quad \text{if } T_{\mathrm{eq}} > 20\,\mathrm{K}. \tag{2.20}$$

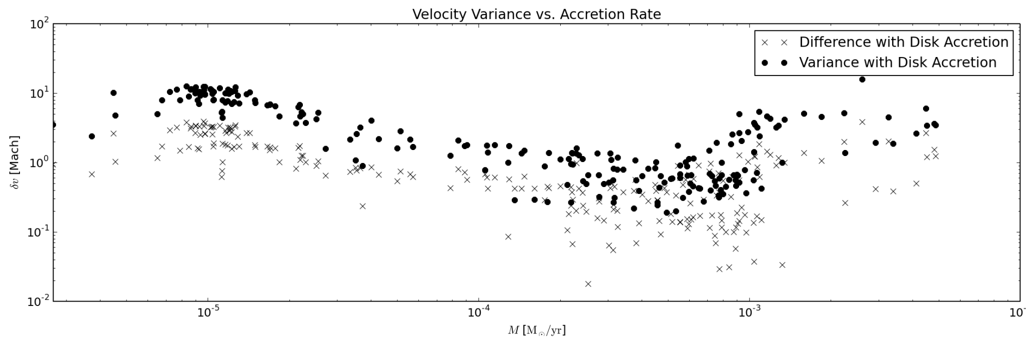

FIGURE 2. Velocity variance and difference from an ideal Keplerian disk in terms of the accretion rate onto the disk.

Finally, the protostar begins to fuse Deuterium on the order of a Kelvin timescale,

$$t_{\mathrm{Kelvin}} \sim 4t_{\mathrm{ff}} \sim 75 \text{ kyr}, \tag{2.21}$$

which instigates dust blow-off and marks the extent of our simulation (Wuchterl & Tscharnuter 2003).

3. Future Work

From logical inferences, the accretion rate effect on disk turbulence in the limit as $\dot{M} \to 0$ becomes negligible, and thus disk laminarization is inevitable; however, this condition is not satisfied until the late protoplanetary stage, which is not simulated here, but is modeled in Chiang & Goldreich (1997). From preliminary low-resolution runs, the evolution of the disk (Figure 1) appears to be approaching this limit, and also indicates a correlation between the accretion rate and the deviation from an ideal Keplerian velocity (Figure 2).

This work will act as a primer to more physical local Spectral simulations looking for *Zombie Vortices* (Marcus *et al.* 2013). The coming results may suggest a more realistic set of initial conditions for local simulations based on the evolutionary stage of interest. We will also be looking for signatures of the drove of Baroclinic instabilities opened up in simulating a now Baroclinic disk.

Support for this work was provided by the US Department of Energy at Lawrence Livermore National Laboratory and the auspices of the Science Undergraduate Research Fellowship granted by the US Department of Energy. The YT software toolkit (Turk *et al.* 2011) was used for data analysis and plotting.

REFERENCES

ALIBERT, Y., MORDASINI, C., BENZ, WILLY & WINISDOER, C. 2005 Models of giant planet formation with migration and disc evolution. *Astronomy and Astrophysics* **353**, 343–353.

BEUTHER, H., LEURINI, S., SCHILKE, P., WYROWSKI, F., MENTEN, K. M. & ZHANG, Q. 2007 Interferometric Multi-wavelength (Sub)millimeter Continuum Study of the Young hHigh-mass Protocluster IRAS 05358+3543. *Astronomy and Astrophysics* **1076**, 1065–1076.

BEUTHER, H., WALSH, A., SCHILKE, P., SRIDHARAN, T. K., MENTEN, K. M. & WYROWSKI, F. 2002 CH3OH and H20 Masers in High-Mass Star-Forming Regions. *Astronomy and Astrophysics* **298**, 289–298.

BOLEY, AARON C., DURISEN, RICHARD H., CAI, KAI, PICKETT, MEGAN K. & ALESSIO, Paola D. 2006 The Thermal Regulation of Gravitational Instabilities in Protoplanetary Disks. III. Simulations with Radiative Cooling and Realistic Opacities. *The Astrophysical Journal* **651**, 517–534.

Chiang, Eugene & Goldreich, P. 1997 Spectral Energy Distributions of T Tauri Stars with Passive Circumstellar Disks. *The Astrophysical Journal* **490**, 368–376.

Ciesla, Fred J. & Cuzzi, Jeffrey N. 2006 The Evolution of the Water Distribution in a Viscous Protoplanetary Disk. *Icarus* **181** (1), 178–204.

Dubinski, John, Narayan, Ramesh & Phillips, T. G. 1995 Turbulence in Molecular Clouds. *The Astronomical Journal* **448**, 226–231.

Evans, Neal J., Dunham, Michael M., Jø rgensen, Jes K., Enoch, Melissa L., Merín, Bruno, van Dishoeck, Ewine F., Alcalá, Juan M., Myers, Philip C., Stapelfeldt, Karl R., Huard, Tracy L., Allen, Lori E., Harvey, Paul M., van Kempen, Tim, Blake, Geoffrey a., Koerner, David W., Mundy, Lee G., Padgett, Deborah L. & Sargent, Anneila I. 2009 The Spitzer c2d Legacy Results: Star-formation rates and efficiencies; evolution and lifetimes. *The Astrophysical Journal Supplement Series* **181** (2), 321–350.

Gammie, Charles F. 2001 Nonlinear outcome of gravitational instability in cooling, gaseous disks. *The Astrophysical Journal* **20** (553), 174–183.

Hansen, Charles E., Klein, Richard I., McKee, Christopher F. & Fisher, Robert T. 2012 Feedback Effects on Low-Mass Star Formation. *The Astrophysical Journal* **747** (1), 22.

Klahr, Hubert H. & Bodenheimer, Peter 2003 Turbulence in Accretion Disks: Vorticity generation and angular momentum transport via the global baroclinic instability. *The Astronomical Journal* **582**, 869–892.

Klein, Richard I. 1999 Star formation with 3-D adaptive mesh refinement : the collapse and fragmentation of molecular clouds. *Journal of Computational and Applied Mathematics* **109**, 123–152.

Krumholz, Mark R., Klein, Richard I., Mckee, Christopher F. & Bolstad, John 2007 Equations and Algorithms for Mixed-Frame Flux-Limited Diffusion Radiation Hydrodynamics. *The Astronomical Journal* **667** (9), 626–643.

Lesur, G. & Papaloizou, J. C. B. 2010 The Subcritical Baroclinic Instability in Local Accretion. *Astronomy and Astrophysics* **513** (A60).

Marcus, Philip S., Pei, Suyang, Jiang, Chung-hsiang & Hassanzadeh, Pedram 2013 Self-Replicating Three-Dimensional Vortices in Neutrally-Stable Stratified Rotating Shear Flows. *Physical Review Letters* **111** (8).

Matsumoto, Tomoaki & Hanawa, Tomoyuki 2003 Fragmentation of a Molecular Cloud Core Versus Fragmentation of the Massive Protoplanetary Disk in the Main Accretion Phase. *The Astrophysical Journal* **3** (2), 913–934.

Matzner, Christopher D & Levin, Yuri 2005 Protostellar Disks: Formation, fragmentation, and the brown dwarf desert. *The Astrophysical Journal* **628** (2), 817–831.

McKee, Christopher F. & Tan, Jonathan C. 2002 Massive star formation in 100,000 years from turbulent and pressurized molecular clouds. *Nature* **416** (6876).

McKee, Christopher F. & Tan, Jonathan C. 2003 The Formation of Massive Stars from Turbulent Cores. *The Astrophysical Journal* **585** (3), 850–871.

Mejia, Annie C., Durisen, Richard H., Pickett, Megan K. & Cai, Kai 2005 The Thermal Regulation of Gravitational Instabilities in Protoplanetary Disks. II. Extended Simulations with Varied Cooling Rates. *The Astrophysical Journal* **619** (2), 1098–1113.

Offner, Stella S. R., Klein, Richard I. & McKee, Christopher F. 2008 Driven and Decaying Turbulence Simulations fo Low-Mass Star Formation: From Clumps to Cores to Protostars. *The Astrophysical Journal* **686** (10), 1174–1194.

Pedlosky, J. P. 1987 *Geophysical Fluid Dynamics*, 2nd edn. New York: Springer.

Rathborne, J. M., Jackson, J. M. & Simon, R. 2006 Infrared Dark Clouds: Precursors to Star Clusters. *The Astrophysical Journal* **641** (1), 389–405.

Rice, W., Lodato, G. & Armitage, Philip J. 2005 Investigating fragmentation conditions in self-gravitating accretion discs. *Monthly Notices of the Royal Astronomical Society: Letters* **364**, 56–60.

Ryu, Dongsu & Goodman, Jeremy 1992 Convective Instability in Differentially Rotating Disks. *The Astrophysical Journal* **388**, 438–450.

Shakura, N. I. & Sunyaev, R. A. 1973 Black Holes in Binary Systems. Observational Appearance. *Astronomy and Astrophysics* **24**, 337–355.

Steiman-Cameron, Thomas Y., Durisen, Richard H., Boley, Aaron C., Michael, Scott & McConnell, Caitlin R 2013 Convergence Studies of Mass Transport in Disks With Gravitational Instabilities. II. the Radiative Cooling Case. *The Astrophysical Journal* **768** (2), 192.

Tritton, D. J. & Davies, P. A. 1985 *Hydrodynamic Instabilities and the Transition to Turbulence*. Berlin: Springer.

Truelove, J. Kelly, Klein, Richard I., McKee, Christopher F., Holliman, John H., Howell, Louis H. & Greenough, Jeffrey A. 1997 The Jeans Condition: A New Constraint on Spatial Resolution in Simulations of Isothermal Self-Gravitational Hydrodynamics. *The Astronomical Journal* **489** (11), L179–L183.

Truelove, J. Kelly, Klein, Richard I., McKee, Christopher F., Holliman, John H., Howell, Louis H., Greenough, Jeffrey A. & Woods, D. Tod 1998 Self-Gravitational Hydrodynamics with Three-Dimensional Adaptive Mesh Refinement: Methodology and Applications to Molecular Cloud Collapse and Fragmentation. *The Astronomical Journal* **495** (3), 821–852.

Turk, Matthew J., Smith, Britton D., Oishi, Jeffrey S., Skory, Stephen, Skillman, Samuel W., Abel, Tom & Norman, Michael L. 2011 yt: A Multi-Code Analysis Toolkit for Astrophysical Simulation Data. *The Astrophysical Journal Supplement Series* **192** (1), 9.

Wuchterl, G. & Tscharnuter, W. 2003 From clouds to stars: Protostellar collapse and the evolution to the pre-main sequence I. Equations and evolution in the Hertzsprung-Russell diagram. *Astronomy and Astrophysics* **398**, 1081–1090.